A 2.3-ps Time-Domain Reflectometer for Millimeter-Wave Network Analysis

Ruai Y. Yu, Masayuki Kamegawa, Michael Case, Mark Rodwell, and Jeff Franklin

Abstract—**A GaAs monolithic time-domain reflectometer (TDR) for millimeter-wave network analysis has been fabricated. The TDR has two outputs from which the incident and reverse waves can be determined. The two channels show 2.3 ps falltime, hence 150 GHz-3 dB TDR bandwidth. The reflection coefficient in the time domain obtained after a partial calibration clearly indicates a prominent reflection when the TDR is under open-circuit load. With the use of network analysis calibration routines, corrected millimeter-wave vector measurements will be feasible with these devices.**

WITH recent work in III-V materials, 350 GHz transistors [1] and 100 GHz MIMIC's [2] have been attained. The device technology has progressed more rapidly than the instrumentation required for device characterization, impairing both the understanding of these devices and the development of circuits incorporating them. Nonlinear transmission lines [3] (NLTL's) and NLTL-gated sampling circuits [4], [5] allow generation and detection of transient signals with ~300 GHz bandwidths. A NLTL-gated directional sampler for network analysis with greater than 10 dB directivity has been demonstrated [5] from 40 to 60 GHz using a microwave frequency sweep source as the stimulus signal. Here we report implementation of an ~150 GHz NLTL-based monolithic time-domain reflectometer (TDR) for millimeter-wave network analysis in which a second NLTL provides a step-function stimulus signal to the device under test. Instead of performing network analysis directly in frequency domain [5], the TDR can be used for the same purpose by Fourier transforming the measured incident and reflected time domain waveforms. Since the stimulus step function in this case contains Fourier components up to ~200 GHz, network analysis at these frequencies is feasible without requiring a swept-frequency millimeterwave source.

The TDR (Fig. 1) consists of a NLTL stimulus signal generator and two modified two-diode bridge sampling circuits [4], [6] placed at the two ports of a 6-dB 50 Ω attenuator (R1–R4). The layout is shown in Fig. 2. A 30 ps strobe step-function is input to a NLTL, which generates a sawtooth waveform with ~2 ps falltime. Symmetric positive and negative impulses are then generated by a balun/differentiator implemented using the coplanar strip (CPS) mode of the input signal coplanar waveguide (CPW). Coupled through R5 and C5, the strobe step-function is applied between the CPW ground planes, and propagates on them in both directions as a CPS mode. 120 μm from the sampling diodes, a short circuit on each side of the CPW ground planes reflects the CPS mode, generating ~3 ps impulses at the sampling

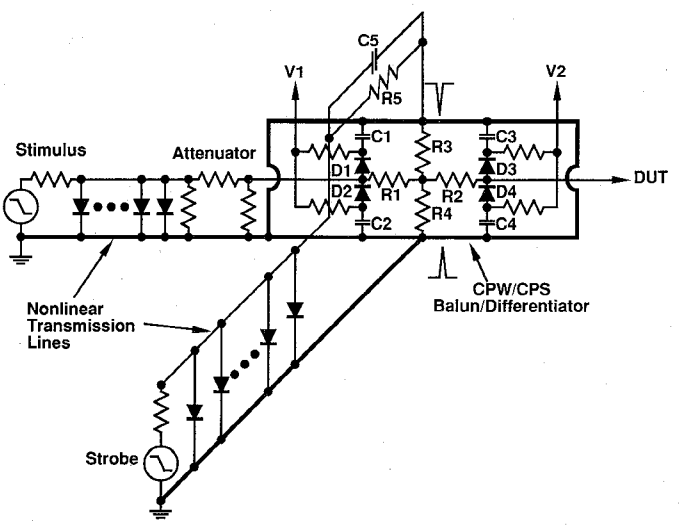

Fig. 1. TDR circuit schematic.

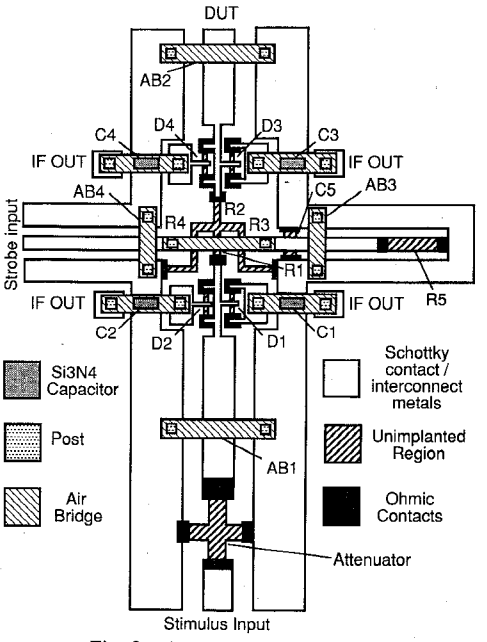

Fig. 2. TDR circuit layout.

Manuscript received June 19, 1991. This work was supported by a National Science Foundation PYI award. Donations for this work came from Tektronix, Hewlett-Packard Corporation, and Hughes Aircraft Corporation.

R. Y. Yu, M. Kamegawa, M. Case, and M. Rodwell are with the Department of Electrical Engineering, University of California, Santa Barbara, Santa Barbara, CA 93106.

J. Franklin is with Varian Associates III-V Device Center, Santa Clara, CA 95054.

IEEE Log Number 9103571.

diodes. A stimulus signal is generated by another NLTL and attenuated to 250 mV by a 25-dB 50 Ω attenuator, thereby providing a small enough signal for linear characterization of transistor circuits; other TDR's were fabricated with 25 mV stimulus signal amplitude, and with on wafer bias tees.

During the sampling aperture time, the complementary strobe impulses drive the sampling diodes (D1–D4) into forward conduction, and the input (RF) signal then partially charges the coupling capacitors (C1–C4). The resulting voltage change is coupled to the sampled output (V_1, V_2) through isolation resistors (not labeled). The RF input signal repetition frequency is offset by Δf from a multiple nf_o of the strobe frequency f_o, and the sampled signal (IF) is then mapped out in equivalent time at a repetition frequency of Δf. Ideally, the forward (V^+) and reverse (V^-) waves can be extracted from the IF signals from the input (IF1) and output (IF2) of the 6-dB attenuator according to the relationships: $V_1 = 2V^+ + V^-/2$, $V_2 = V^+ + V^-$, hence, $V^+ = (1/3)(2V_1 - V_2)$, $V^- = (2/3)(2V_2 - V_1)$.

The TDR is implemented in a six-mask process. Starting with a semi-insulating GaAs substrate, a heavily doped ($6 \times 10^{18}/\text{cm}^3$, 1 μm thickness) $N+$ layer is grown by molecular beam epitaxy. This serves as the diode cathode connection. A surface $N-$ active layer (425 nm thickness), with an exponentially-graded hyperabrupt doping profile ($2 \times 10^{17}/\text{cm}^3$ surface doping, 225 nm grading constant), is then grown. Ohmic contacts to the $N+$ layer are formed by a 0.5 μm recess etch through the $N-$ layer, a self-aligned AuGe–Ni–Au liftoff, and a subsequent rapid thermal anneal. Measured contact resistance and $N+$ layer sheet resistance are 30 Ω-μm and 9 Ω per square. Proton implantation converts the $N+$ and $N-$ layers to semi-insulation material, determining diode junction areas and defining resistors in the $N+$ layer. A dual-energy implant, at 180 keV ($1.7 \times 10^{15}/\text{cm}^2$) and 110 keV ($4 \times 10^{14}/\text{cm}^2$), is used to penetrate the combined $N+$ and $N-$ layers. During implantation, the diode regions and resistors are protected by a 1.6 μm Au on polyimide mask. Interconnections are formed with a 800 Å Ti–800 Å Pt–11000 Å Au liftoff; Schottky contacts result where the metal intersects unimplanted material.

The coupling capacitors (C1–C4) are implemented using 850 Å Si_3N_4 films. The small compensation capacitor (C5) was implemented using reverse-biased diode. Adaptation of electroplated air bridges (AB) for cross-over of signal lines greatly simplifies the circuit layout and minimizes circuit parasitics. AB1 and AB2 provide the short circuits for the balun/differentiator, while AB3 and AB4 provide continuity for the stimulus signal CPW ground planes.

The TDR risetime is determined by the signal line RC time constant and by the sampling diode aperture time. The four sampling diode parasitics load the RF line with 16 fF capacitance at both the attenuator input and output, limiting the bandwith. Aperture time is determined by the strobe pulse duration and by the sampling diode reverse bias relative to the strobe pulse peak voltage [3].

As described in [4], compensation capacitor C5 permits high differentiator efficiency, while maintaining a low reflection termination to the NLTL. Depending upon diode reverse bias, ~1 ps aperture time and ~2 ps RF line risetime are expected. The predicted TDR falltime is then $T_{TDR} = \sqrt{1^2 + 2^2} = 2.2$ *ps*, corresponding to a 160 GHz 3-dB bandwidth. The linear input range is predicted to be ±1 *V* by SPICE simulation.

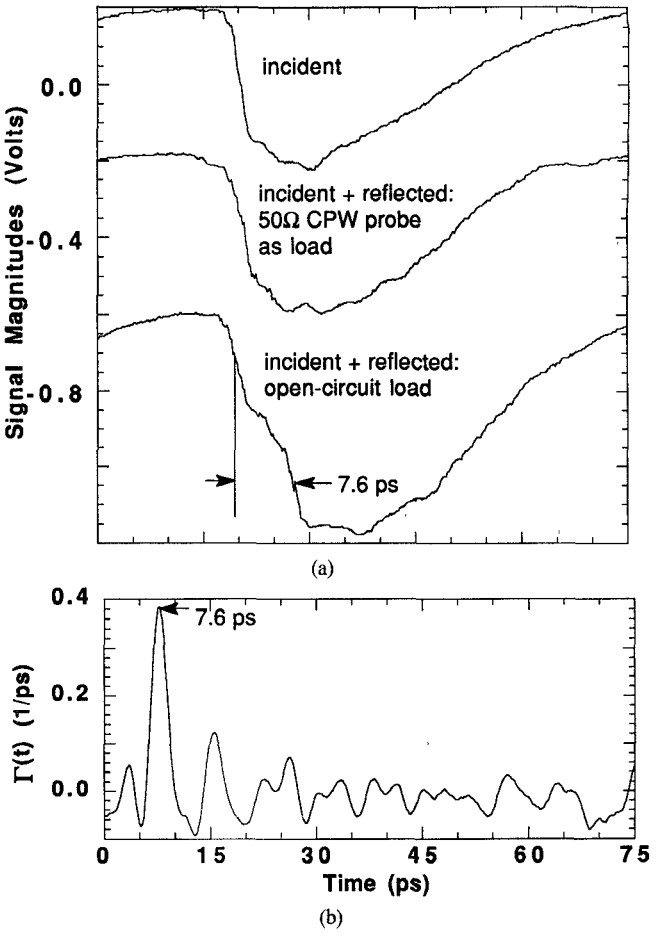

Fig. 3. (a) Observed TDR waveforms: incident wave, and (incident + reflected) waves with the TDR open-circuited or connected to a terminated 40 GHz microwave wafer probe. (b) Reflection coefficient displayed in time with the TDR open-circuited.

In measuring the TDR performance, synchronized microwave synthesizers drove the strobe NLTL at 14 GHz, 27 dBm and the stimulus signal NLTL at 14 GHz + 140 Hz, 25 dBm, resulting in a 140 Hz IF output. Resulting TDR waveforms both under an open circuit and a 40 GHz 50 Ω CPW probe as a load are shown in Fig. 3(a). The distinct two step response under open circuit clearly indicates the reflection from the open circuit, and the 7.6 ps delay of the reflected step corresponds to the expected round-trip time between the directional sampler and the TDR test port. The falltime of the steps was measured to be 2.3 ps, corresponding to a 150 GHz TDR bandwidth.

For calibrated reflection measurements, three calibration standards must be used, but these were not available for millimeter-wave frequencies. To demonstrate the TDR, a partially-calibrated measurement was performed on an open-circuit termination. The sampling diode and layout parasitics load the network R1–R4, and its attenuation $H(\omega)/2$ then varies with frequency. Hence, $V_2(\omega) = V^+(\omega) + V^-(\omega)$

and $V_1(\omega) = 2V^+(\omega)/H(\omega) + H(\omega)V^-(\omega)/2$. By measuring $V_{1,50\Omega}(\omega)$ and $V_{2,50\Omega}(\omega)$ with the test port loaded by a 40 GHz coplanar microwave probe and coaxial termination, $H(\omega) = 2V_{2,50\Omega}(\omega)/V_{1,50\Omega}(\omega)$ is determined. The reflection coefficient of an arbitrary load is then found from

$$\Gamma(\omega) = \frac{2V_2(\omega) - H(\omega)V_1(\omega)}{H(\omega)\left(V_1(\omega) - H(\omega)V_2(\omega)/2\right)}.$$

After calibration, $V_1(\omega)$ and $V_2(\omega)$ were measured with an open-circuit termination. The resulting $\Gamma(\omega)$ was numerically low-pass-filtered by a 190 GHz 3-dB bandwidth Gaussian filter (2.2 ps FWHM impulse response) to bandlimit high-frequency noise, and inverse Fourier transformed to obtain $\Gamma(t)$. The resulting $\Gamma(t)$ for an open-circuit at the TDR test port is shown in Fig. 3(b), with a major reflection of $0.38 \cdot (1/ps)$ peak amplitude, and 2.6 ps FWHM duration observed at the expected 7.6 ps round-trip delay. The product of magnitude and reflection duration yields a dc reflection coefficient of $(1.06)(0.38/ps)(2.6\ ps) = 1.05$, with the factor of 1.06 arising from an assumed Gaussian pulse shape.

The rudimentary calibration procedure above does not correct for the TDR source reflection coefficient and uses a 40 GHz microwave wafer probe and termination as a calibration standard over a 14 GHz -190 GHz bandwidth. These errors introduce the additional structure seen in $\Gamma(t)$ (Fig. 3(b)). In particular, we ascribe the second peak in $\Gamma(t)$ at 15.2 ps (2×7.6 ps) to the uncorrected TDR source reflection coefficient.

In conclusion, we have successfully fabricated a NLTL-based TDR with ~ 150 GHz 3-dB bandwidth. Directionality of the TDR is demonstrated by the clear indication of open circuit reflections. Incorporating these devices, and with the use of Fourier transform and network analysis calibration routines, active coplanar probes [7] for millimeter-wave on-wafer network analysis can be developed due to the wide spectral content available from the stimulus signal and the wide bandwidth of the directional sampling circuit.

References

[1] U. K. Mishra, A. S. Brown, and S. E. Rosenbaum, "DC and RF performance of 0.1 μm gate length AlInAs-GaInAs pseudo-morphic HEMT's," *Tech. Dig., 1988 Int. Electron Device Meeting,* San Francisco, CA, Dec. 4–11, 1988.

[2] R. Majidi-Ahy, C. Nishimoto, M. Riaziat, M. Glenn, S. Silverman, S. Weng, Y. Pao, G. Zdasiuk, S. Bandy, and Z. Tan," 100 GHz high-gain InP MMIC cascode amplifier," *1990 GaAs IC Symp.,* New Orleans, LA, Oct. 7–10, 1990.

[3] M. J. W. Rodwell, M. Kamegawa, R. Yu, M. Case, E. Carman, and K. S. Kiboney, "GaAs nonlinear transmission lines for picosecond pulse generation and millimeter-wave sampling," *IEEE Trans. Microwave Theory Tech.,* vol. 39, pp. 1194–1204, July 1991.

[4] R. Y. Yu, M. Case, M. Kamegawa, M. Sundaram, M. J. W. Rodwell, and A. W. Gassard, "275 GHz 3-mask integrated GaAs sampling circuit," *Electron. Lett.,* vol. 26, no. 13, June 21, 1990.

[5] R. A. Marsland, C. J. Madden, D. W. Van Der Weide, M. S. Shakouri, and D. M. Bloom, " Monolithic integrated circuits For MM-wave instrumentation," *1990 GaAs IC Symp.* New Orleans, LA, Oct. 7–10, 1990.

[6] W. M. Grove, "A dc to 12.4 GHz feedthrough sampler for oscilloscopes and other RF systems," *Hewlett-Packard J.,* Oct. 1966.

[7] R. Majidi-Ahy and D. M. Bloom, "120 GHz active wafer probes for picosecond device measurement," *Proc. Picosecond Electron. Optoelectron.,* Salt Lake City, UT, Mar. 1989.